AD-A035 224 PENNSYLVANIA STATE UNIV UNIVERSITY PARK APPLIED RESE--ETC F/G 10/1
RESILIENT MOUNTING OF MACHINERY ON PLATELIKE AND MODIFIED PLATE--ETC(U)
NOV 76 J C SNOWDON N00017-73-C-1418
UNCLASSIFIED TM-76-278 NL

1 OF 1
AD
A035224

END
DATE
FILMED
3-77

ADA035224

1

(12)

B.S.

RESILIENT MOUNTING OF MACHINERY ON PLATELIKE
AND MODIFIED PLATELIKE SUBSTRUCTURES (U)

J. C. Snowdon

Technical Memorandum
File No. TM 76-278
November 2, 1976
Contract No. N00017-73-C-1418

Copy No. 58

The Pennsylvania State University
Institute for Science and Engineering
APPLIED RESEARCH LABORATORY
P. O. Box 30
State College, PA 16801

NAVY DEPARTMENT

NAVAL SEA SYSTEMS COMMAND

This investigation was sponsored by the Naval Sea Systems Command, Ship Silencing Division, and the Office of Naval Research.

UNCLASSIFIED

SECURITY CLASSIFICATION OF THIS PAGE (When Data Entered)

REPORT DOCUMENTATION PAGE

READ INSTRUCTIONS BEFORE COMPLETING FORM

1. REPORT NUMBER: 14 TM-76-278
2. GOVT ACCESSION NO.
3. RECIPIENT'S CATALOG NUMBER: 9

4. TITLE (and Subtitle): 6 Resilient Mounting of Machinery on Platelike And Modified Platelike Substructures. (U)

5. TYPE OF REPORT & PERIOD COVERED: Technical memo.

6. PERFORMING ORG. REPORT NUMBER

7. AUTHOR(s): 10 J. C. Snowdon

8. CONTRACT OR GRANT NUMBER(s): 15 N00017-73-C-1418

9. PERFORMING ORGANIZATION NAME AND ADDRESS:
The Pennsylvania State University
Applied Research Laboratory
P. O. Box 30, State College, PA 16801

10. PROGRAM ELEMENT, PROJECT, TASK AREA & WORK UNIT NUMBERS: 62543N
SF 43-452-702 (NavSea)
N00014-76-RQ-00002 (ONR)

11. CONTROLLING OFFICE NAME AND ADDRESS:
Naval Sea Systems Command, Department of the Navy, Washington, DC 20362
Office of Naval Research, Department of the Navy, Arlington, VA 22217

12. REPORT DATE: 11 2 Nov[redacted] 1976

13. NUMBER OF PAGES: 37

14. MONITORING AGENCY NAME & ADDRESS (if different from Controlling Office): 12 38p.

15. SECURITY CLASS. (of this report): UNCLASSIFIED

15a. DECLASSIFICATION/DOWNGRADING SCHEDULE

16. DISTRIBUTION STATEMENT (of this Report): 16 F43452

Approved for public release; distribution unlimited.
Per NAVSEA November 15, 1976.

17 SF43452702

17. DISTRIBUTION STATEMENT (of the abstract entered in Block 20, if different from Report)

18. SUPPLEMENTARY NOTES

19. KEY WORDS (Continue on reverse side if necessary and identify by block number)

Vibration isolation.
Antivibration mountings.
Machinery vibration.
Platelike substructures.
Dynamic vibration absorbers.

20. ABSTRACT (Continue on reverse side if necessary and identify by block number)

The problem of isolating machinery vibration from platelike substructures is analyzed. Simply supported, internally damped, square rectangular, and circular plates are considered, as are rectangular plates with rigid cross members that divide the plates into separate quadrants. The machinery is supported either by eight or by four antivibration mounts located symmetrically about the plate centers. The attachment of dynamic vibration absorbers or lumped masses to the plates at each mount location

LB

DD FORM 1 JAN 73 1473 EDITION OF 1 NOV 65 IS OBSOLETE

UNCLASSIFIED

SECURITY CLASSIFICATION OF THIS PAGE (When Data Entered)

391 007

20. is shown to be effective in reducing the force transmitted to the plate boundaries. The dynamic absorbers are tuned to suppress transmissibility at the fundamental resonance of the plate of concern, whereas the lumped masses become effective at frequencies above this resonance where their impedance predominates that of the plate. Utilization of the circular and quadrant plates greatly reduces the number of plate resonances that contribute to the force transmitted to the plate boundaries. Further, when machinery is supported by four antivibration mounts on square and rectangular plates, the number of resonances that are excited can also be reduced significantly if the mount locations are chosen judiciously. However, the use of other mount locations can yield a large number of pronounced resonances in excess of those excited when the machinery is supported by various arrangements of eight antivibration mounts--for which transmissibility does not appear to change greatly with the choice of mount location.

ABSTRACT

The problem of isolating machinery vibration from platelike substructures is analyzed. Simply supported, internally damped, square, rectangular, and circular plates are considered, as are rectangular plates with rigid cross members that divide the plates into separate quadrants. The machinery is supported either by eight or by four antivibration mounts located symmetrically about the plate centers. The attachment of dynamic vibration absorbers or lumped masses to the plates at each mount location is shown to be effective in reducing the force transmitted to the plate boundaries. The dynamic absorbers are tuned to suppress transmissibility at the fundamental resonance of the plate of concern, whereas the lumped masses become effective at frequencies above this resonance where their impedance predominates that of the plate. Utilization of the circular and quadrant plates greatly reduces the number of plate resonances that contribute to the force transmitted to the plate boundaries. Further, when machinery is supported by four antivibration mounts on square and rectangular plates, the number of resonances that are excited can also be reduced significantly if the mount locations are chosen judiciously. However, the use of other mount locations can yield a large number of pronounced resonances in excess of those excited when the machinery is supported by various arrangements of eight antivibration mounts--for which transmissibility does not appear to change greatly with the choice of mount location.

INTRODUCTION

Considered here is the resilient mounting of a vibrating item of machinery of mass M on platelike substructures that have been modeled as thin, simply supported, square, rectangular, or circular plates with small internal damping. Also considered are plates that have been modified by the attachment of dynamic vibration absorbers or lumped masses at each mount location--or by the introduction of rigid cross members, which divide the square and rectangular plates into four separate quadrants that are free to vibrate independently of one another.

The item of machinery is supported either by eight or by four antivibration mounts that are arbitrarily, but symmetrically, located with respect to the plate centers. The mounts have complex stiffnesses K^* and small internal damping factors δ_K governed by the equation

$$K^* = K(1 + j\delta_K) \quad , \tag{1}$$

where $j = \sqrt{-1}$ and K is the real part and δ_K is the ratio of the imaginary to the real part of K^*.[1] Mount damping is of the Solid Type I; that is, the frequency dependence of K and δ_K is assumed to be negligible.[2]

A vibratory force $\tilde{F}_1$ acts vertically on the mounted item to produce a total vertical force $\tilde{F}_2$ at the plate boundaries. For each of the plate configurations mentioned in the foregoing, transmissibility $T = |\tilde{F}_2/\tilde{F}_1|$ has been calculated in terms of a frequency ratio $\Omega = \omega/\omega_0$, where ω is the impressed angular frequency, hereafter referred to simply as frequency, and ω_0 is the natural frequency of the mounting system calculated as though the platelike substructures were ideally rigid. The overall transmissibility levels may appear to be low at high frequencies, but it should be recognized that even small amounts of vibratory energy can excite the natural modes of neighboring, and sometimes of distant, platelike structures. Many of these plate modes will be efficient radiators of unwanted noise.

1. SQUARE PLATES

An item of machinery supported by eight identical antivibration mounts on a rectangular plate of mass M_p and sides of lengths a and μa is shown in Fig. 1(a). For a square plate, the parameter $\mu = 1.0$. The symmetric mount locations are specified by coordinates (h_{1x},h_{1y}), (h_{2x},h_{2y}) that describe the distance of two adjacent mounts on one side of the machine from the near plate corner, which is taken as the coordinate origin.

The force transmissibility T across the mounting system (Introduction) can be expressed as follows:

$$T = \left| \frac{U^* V^*}{[1 - (\Omega^*)^2 - W^*]} \right| \quad , \tag{2}$$

where

$$U^* = \sum_{k=1,3,5\ldots}^{\infty} \; \sum_{m=1,3,5,\ldots}^{\infty} \frac{16(\beta^*)^4}{\pi^2 k m \lambda^*} [\varphi_{k,m}(h_{1x},h_{1y}) + \Gamma^* \varphi_{k,m}(h_{2x},h_{2y})] \quad , \tag{3}$$

$$V^* = \frac{(1 - B^* + C^*)}{2[(1 + A^*)(1 + C^*) - (B^*)^2]} \quad , \tag{4}$$

$$W^* = \frac{(A^* + 2B^* + C^*) + 2[A^*C^* - (B^*)^2]}{2[(1 + A^*)(1 + C^*) - (B^*)^2]} \quad , \tag{5}$$

and

$$(\Omega^*)^2 = \Omega^2/(1 + j\delta_K) = (\omega/\omega_o)^2/(1 + j\delta_K) \quad . \tag{6}$$

In these equations,

$$A^* = \sum_{k=1,3,5,\ldots}^{\infty} \; \sum_{m=1,3,5,\ldots}^{\infty} \frac{2\gamma \; \varphi^2_{k,m}(h_{1x},h_{1y})}{\lambda^*(\Omega^*)^2} \quad , \tag{7}$$

$$B^* = \sum_{k=1,3,5,\ldots}^{\infty} \; \sum_{m=1,3,5,\ldots}^{\infty} \frac{2\gamma \; \varphi_{k,m}(h_{1x},h_{1y}) \; \varphi_{k,m}(h_{2x},h_{2y})}{\lambda^*(\Omega^*)^2} \quad , \tag{8}$$

$$C^* = \sum_{k=1,3,5,\ldots}^{\infty} \; \sum_{m=1,3,5,\ldots}^{\infty} \frac{2\gamma \; \varphi^2_{k,m}(h_{2x},h_{2y})}{\lambda^*(\Omega^*)^2} \quad , \tag{9}$$

$$\Gamma^* = \left|\frac{1 + A^* - B^*}{1 - B^* + C^*}\right| \quad , \tag{10}$$

$$\varphi_{k,m}(h_{ix},h_{iy}) = \sin k\pi(h_{ix}/a) \sin m\pi(h_{iy}/\mu a) \; , \qquad (i = 1,2) \quad , \tag{11}$$

$$\lambda^* = [(\beta^*)^4 - 1] \quad , \tag{12}$$

and

$$\beta^* = \left(\frac{n_{k,m}a}{n^* a}\right) = \frac{\pi[k^2 + (m/\mu)^2]^{\frac{1}{2}}}{(p + jq)} \quad , \tag{13}$$

where

$$\gamma = M/M_p \quad . \tag{14}$$

If the damping factors δ_E and δ_G associated with the Young's modulus and shear deformations of the plate material are equal, as may realistically be assumed,[2-4] then the Poisson's ratio of the plate will be a real rather than a complex quantity, and the parameters p and q of Eq. 13 describe the real and imaginary parts of the parameter

$$(n^* a) = na/(1 + j\delta_E)^{\frac{1}{2}} \quad , \tag{15}$$

where n^* is the complex wavenumber of the plate.[5] It can be shown that

$$p = na \left[\frac{1}{2\sqrt{D_E}} + \frac{(1 + D_E)^{\frac{1}{2}}}{2\sqrt{2}\, D_E}\right]^{\frac{1}{2}} \quad . \tag{16}$$

and

$$q = -na \left[\frac{1}{2\sqrt{D_E}} - \frac{(1 + D_E)^{\frac{1}{2}}}{2\sqrt{2}\, D_E}\right]^{\frac{1}{2}} \quad , \tag{17}$$

where

$$D_E = (1 + \delta_E^2)^{\frac{1}{2}} \quad . \tag{18}$$

Finally, the frequency ratio Ω and the dimensionless product na are related as follows:

$$\Omega = \frac{(na/2)^2 \Xi}{N_{R1}^2} \quad , \tag{19}$$

where

$$N_{R1} = \pi \sqrt{(1 + \mu^2)/2\mu} \tag{20}$$

is the value taken by (na/2) at the fundamental resonant frequency ω_{11} of the unloaded plate, and

$$\Xi = \omega_{11}/\omega_o \quad . \tag{21}$$

Odd integral values of k and m appear in the summations of Eqs. 3 and 7-9 because only the symmetrical plate modes contribute to plate transmissibility.[5] Whereas forces are transmitted to the plate boundaries when the antisymmetric modes are excited (k and m even), the net upward and downward components of these forces counter one another exactly. Values of k and m through a range of at least 1-99 have been employed in all summations evaluated here.

When the item of machinery is supported by only four antivibration mounts, as in Fig. 1(b), $h_{1x} = h_{2x}$, and $h_{1y} = h_{2y}$, so that Eqs. 7-9 for A^*, B^*, and C^* become identical; and the expression for transmissibility reduces to

$$T = \left| \frac{T^*}{[1 - (\Omega^*)^2 - \gamma\xi^*]} \right| \quad , \tag{22}$$

where

$$T^* = \sum_{k=1,3,5,\ldots}^{\infty} \sum_{m=1,3,5,\ldots}^{\infty} \frac{16(\beta^*)^4 \varphi_{k,m}(h_x,h_y)}{\pi^2 km\lambda^*} \tag{23}$$

and

$$\xi^* = \sum_{k=1,3,5,\ldots}^{\infty} \sum_{m=1,3,5,\ldots}^{\infty} \frac{4\varphi^2_{k,m}(h_x,h_y)}{\lambda^*} \quad . \tag{24}$$

Note that, for the system of Fig. 1(a), the natural mounting frequency ω_o (Introduction and Eq. 6) is defined as

$$\omega_o = (8K/M)^{\frac{1}{2}} \quad ; \tag{25}$$

whereas, for the system of Fig. 1(b),

$$\omega_o = 2(K/M)^{\frac{1}{2}} \quad . \tag{26}$$

Plotted in Fig. 2 are the results of transmissibility calculations made from Eq. 2 for a vibrating machine supported by eight mounts on a square plate ($\mu = 1.0$) having the relatively small damping factors $\delta_E = \delta_G = 0.01$. The mounts are uniformly spaced such that $h_{1x} = 0.2a$, $h_{2x} = 0.4a$, and $h_{1y} = h_{2y} = a/3$; here, and subsequently, the mount damping factors $\delta_K = 0.05$. The mass and frequency ratios are $\gamma = M/M_P = 4$ and $\Xi = \omega_{11}/\omega_o = 4$. The transmissibility when the plate is ideally rigid is shown by the dashed curve. Note that the first transmissibility peak (solid curve) occurs at a smaller value of the frequency ratio $\Omega = \omega/\omega_o$ than unity because the effective stiffness of the mounts is reduced by the plate flexibility. Again, the second peak occurs at a greater value of Ω than 4 because the natural frequencies of the plate are shifted to higher frequencies by the springlike constraint exerted by the mounts.

The transmissibility curve of Fig. 2 is characterized by many resonances as compared to curves that have been calculated for an item of machinery supported by beamlike and modified beamlike substructures.[6] Furthermore, the curve of Fig. 2 is typical of many other curves that have been calculated for a variety of mount locations. For example, no advantage existed to deploying the eight mounts in circular configurations of different radii and equal angular spacings about the plate center. Nor could customary linear mount configurations be found that provided noticeably reduced numbers or levels of transmissibility peaks.

By contrast, judicious choice of mount locations is possible when an item of machinery is supported by only four mounts, and results comparable to those of Fig. 2 can be obtained. Unfortunately, the use of other, less favorable, mount locations can then greatly increase the extent to which the plate resonances are excited. This is evident in Fig. 3, which relates to the same square plate as before and to four mounts having symmetrical locations specified by $h_x/a = h_y/a = 0.25$. The mass and frequency ratios $\gamma = \Xi = 4$ remain unchanged in value. The transmissibility curve is now far more "spiky" than in Fig. 2, and the plate will respond more strongly than before to the amplitudes of the disturbing frequencies from the mounted item. However, by contracting the mount separation until $h_x/a = h_y/a = 1/3$, the transmissibility curve of Fig. 4 is obtained with a smaller density of resonances; in fact, this judicious choice of mount locations has halved the number of plate resonances that are excited. Thus, excitation by an impressed force of any mode of plate vibration, other than the first, can be avoided[5] if the force is located at any <u>point</u> on a nodal <u>line</u> of the particular mode of concern.

This fact has been used to advantage in the present situation, where each of the four mounts is located on nodal lines of the [(3,1),(1,3)], (3,3), [(5,3),(3,5)], [(7,3,),(3,7)],..., modes, which ar_ no longer excited; rather, only the following sequence of symmetrical modes is observed: (1,1), [(5,1),(1,5)], [(7,1),(1,7),(5,5)], [(7,5),(5,7)],... .

2. CIRCULAR PLATES

The possibility has been examined of mounting machinery on circular platelike floor areas. Such an area, for example, could be supported around its perimeter by a rigid circular rib and be separated by an expansion joint from the adjacent floor areas of the square or rectangular machinery room in which it is located. This situation is modeled in Fig. 5(a), where a simply supported circular plate is excited symmetrically by four, equal, in-phase vibratory forces. The forces are transmitted from an item of machinery of mass M by mounts of equal stiffness that are located on the plate at equal distances $\lambda a'$ from the plate center, where a' is the plate radius (and, thus, the <u>half-length</u> of the sides of the circumscribing square). The parameter λ, which should not be confused with the complex quantity of Eq. 12, is chosen such that $0 < \lambda < 1.0$.

The force transmissibility T across the mounting system to the plate boundaries is governed by the equation

$$T = |\Psi^*/[1 - (\Omega^*)^2 + \Theta^*]| \quad , \tag{27}$$

where

$$\Theta^* = \gamma(n^* a')\, \Phi^*/\lambda \quad , \tag{28}$$

$$\Psi^* = \left[\frac{(J_{o\lambda}I_o + I_{o\lambda}J_o) - \phi^*_{a'}(J_{o\lambda}I_1 + I_{o\lambda}J_1)}{2J_oI_o - \phi^*_{a'}(J_oI_1 + J_1I_o)}\right]_{(n^*a')} \quad , \tag{29}$$

and Ω^* is again given by Eq. 6 in which

$$\Omega = (na')^2\Xi/(2.2325)^2 \quad . \tag{30}$$

As before, $\Xi = \omega_{11}/\omega_o$, where ω_{11} is now the fundamental resonant frequency of the circular plate of mass M_p. In addition, $\gamma = M/M_p$, and

$$\phi^* = R^*/S^* \quad , \tag{31}$$

where

$$R^* = \lambda\{2\Lambda\phi^*_{a'}(J_{o\lambda}I_{o\lambda}) - (n^*a')(J_{o\lambda}Y_{o\lambda}+\Lambda K_{o\lambda}I_{o\lambda})[\phi^*_{a'}(J_1I_o + J_oI_1)-2J_oI_o]$$

$$+ (n^*a')(J_{o\lambda})^2[\phi^*_{a'}(Y_1I_o+I_1Y_o)-2Y_oI_o] + \Lambda(n^*a')(I_{o\lambda})^2[\phi^*_{a'}(J_1K_o-K_1J_o)-2J_oK_o]\}_{(n^*a')} \tag{32}$$

and

$$S^* = -4\,\Lambda[\phi^*_{a'}(J_1I_o + J_oI_1) - 2J_oI_o]_{(n^*a')} \quad . \tag{33}$$

In these equations, such abbreviations as J_o, I_1, $Y_{o\lambda}$, and $K_{o\lambda}$ have been used to represent the ordinary and modified Bessel functions $J_o(n^*a')$, $I_1(n^*a')$, $Y_o(\lambda n^*a')$, and $K_o(\lambda n^*a')$; in addition

$$\Lambda = 2/\pi \tag{34}$$

and

$$\phi^*_{a'} = (1 - \nu)/(n^* a') \quad , \tag{35}$$

where ν is Poisson's ratio. All Bessel functions have the complex argument n^*a', a dimensionless product that is given by Eqs. 15-18 in which the quantity a is currently replaced by the plate radius a'.

Selection of the values $\lambda = 0.4714$ and 0.7071 yields mount locations that are congruent to those utilized on the square plates considered in Figs. 4 and 3, where $h_x/a = h_y/a = 1/3$ and 1/4, respectively. For example, the solid transmissibility curve of Fig. 6 has been calculated from Eq. 27 with the mass and frequency ratios $\gamma = \Xi = 4$ and the plate damping factors $\delta_E = \delta_G = 0.01$, as before, and with mount locations specified by the value $\lambda = 0.7071$. Although these mount locations were previously associated with a pronounced resonant response of the square plate considered in Fig. 3, only one-third of the number of resonant peaks is now in evidence. Moreover, the dashed curve of Fig. 6 shows how the mount spacing can be contracted to avoid the excitation of the second symmetrical plate resonance; thus, because the mounts now lie on the single nodal circle (for which $\lambda = 0.4414$) accompanying this resonance, the normally anticipated transmissibility peak ($\Omega \simeq 25$) has been replaced by a broad trough of significantly lower level.

To conclude, it should be recognized that a favorable example has been considered in the foregoing, and that the overall reduction in the number of plate resonances excited would be much smaller had comparison been made, for example, between transmissibility curves calculated (1) for the judicious mount locations chosen on the square plate considered in Fig. 4, and (2) for the corresponding mount locations ($\lambda = 0.4714$) on the circular plate. This is not because the adoption of the circular plate would be ineffective but, rather, because the judicious choice of mount locations had proved extremely effective in the first instance.

3. QUADRANT PLATES

The possibility of mounting machinery on divided plates has also been examined. Thus, in Fig. 5(b) a rectangular plate is cut by expansion joints into four identical quadrants that are supported by ideally rigid cross members. Each quadrant is assumed to have simply supported boundaries, to be free to vibrate independently of the other three quadrants, and to be driven solely by the force transmitted by a single antivibration mount. The four impressed forces of Fig. 5(b) are assumed to have equal magnitude and phase, as in Fig. 5(a) and Sec. 2, and to be symmetrically located. Because the quadrants have a fundamental resonant frequency that is four times higher than that of the undivided plate, the vibration levels and the transmitted forces at this fundamental resonance, and at higher resonances, will be reduced significantly because the antivibration mounts will have greater effectiveness at these higher frequencies.

If transmissibility T is defined as the total magnitude of the output forces at the boundaries of the quadrants divided by a force $\tilde{F}_1$ impressed as in Fig. 1(b), and if the quadrant sides have the lengths $a' = a/2$ and $\mu a' = \mu a/2$, then it can be verified that

$$T = \left| \frac{(T^*)'}{[1 - (\Omega^*)^2 - \gamma(\xi^*)']} \right| , \tag{36}$$

where $(T^*)'$ and $(\xi^*)'$ are given by Eqs. 23 and 24 in which β^* and $\varphi_{k,m}(h_x,h_y)$ have been replaced by

$$(\beta^*)' = \frac{\pi[k^2 + (m/\mu)^2]^{\frac{1}{2}}}{(n^* a')} \tag{37}$$

and

$$\varphi_{k,m}(h_{x'},h_{y'}) = \sin k\pi(h_{x'}/a') \sin m\pi(h_{y'}/\mu a') \quad . \tag{38}$$

In Eq. 38, the coordinates $h_{x'}$ and $h_{y'}$ describe the distance of the mounting point on the lower left-hand quadrant plate of Fig. 5(b) from the near plate corner. In addition, the summations of Eq. 24 now encompass every integral value of $k,m = 1,2,3,\ldots$, the parameter Ω^* is defined by Eq. 6 in which

$$\Omega = \frac{(na')^2\Xi}{N_{R1}^2} \quad , \tag{39}$$

and $\gamma = M/M_p$. Here, as before, the mass M_p, the quantity N_{R1} (Eq. 20), and the frequency ratio $\Xi = \omega_{11}/\omega_o$, relate to the undivided plate having sides of lengths a and μa. Finally, the parameter (n^*a') in Eq. 37 is specified by Eqs. 15-18 in which a is replaced by $a' = a/2$.

Transmissibility calculations that have been made from Eq. 36 for a square plate ($\mu = 1.0$) having square quadrants are plotted in Fig. 7. For both curves of this figure, the mass and frequency ratios $\gamma = \Xi = 4$; the plate damping factors $\delta_E = \delta_G = 0.01$, as in all previous calculations. The mounts are also located as they were on the undivided plates. Thus, the solid and dashed curves have been calculated for $h_{x'}/a' = h_{y'}/a' = 1/2$ and $2/3$ -- values for which the mount locations match those utilized in Figs. 3 and 4, respectively. The fundamental resonance of the quadrant plates is seen to occur at a frequency that is essentially four times higher than that of the fundamental plate resonance evident in the prior figures; namely, it occurs where $\Omega \approx 16$, as expected. Moreover, for both mount locations, the quadrant-plate resonances excited are only one third as numerous as the resonances evident in Figs. 3 and 4 through the same frequency range of calculation.

The judicious mount locations of Fig. 4 have remained equally effective in Fig. 7 and have resulted in the appearance in the dashed curve of only three quadrant-plate resonances, except for minute responses from the [(2,1),(1,2)], (2,2) modes where $\Omega \approx 40$ and 64. (These modes, which are nonsymmetrical, would not be excited were the quadrant plates unconstrained by the antivibration mounts.) Effectively, then, only the (1,1), [(5,1), (1,5)], and [(7,1),(1,7),(5,5)] modes of the quadrant plates give rise to resonances in the dashed curve of Fig. 7, and the excitation of the [(3,1), (1,3)], (3,3), and [(5,3),(3,5)] modes at intervening frequencies has been avoided because the antivibration mounts have been located at points on nodal lines of these modes. Although the predicted performance of the quadrant plates does require that the supporting cross members [Fig. 5(b)] remain rigid, the use of such plates appears to represent one effective approach to mounting machinery on platelike floor areas.

4. RECTANGULAR PLATES

Rectangular plates having identical aspect ratios $\mu = 1/2$ are considered in this final Section. The effectiveness of mounting machinery on quadrant plates is illustrated again in Fig. 8. The value of attaching dynamic vibration absorbers or lumped masses to undivided plates at each mount location is demonstrated subsequently.

The transmissibility curves of Fig. 8 have been determined for new values of the mass and frequency ratios $\gamma = M/M_p = 6$ and $\Xi = \omega_{11}/\omega_o = 5$, and for values of the mount and plate damping factors $\delta_K = 0.05$ and $\delta_E = \delta_G = 0.01$ that will be utilized throughout this Section. The solid curve relates to the mounting configuration of Fig. 1(a), where eight antivibration mounts are uniformly spaced beneath the item of machinery such that $h_{1x} = 0.2a$, $h_{2x} = 0.4a$, and $h_{1y} = h_{2y} = \mu a/3 = a/6$. The dashed curve shows how the number of transmissibility peaks can be reduced significantly if four antivibration mounts are deployed on the quadrant plates of Fig. 5(b) such that $h_{x'} = 2a'/3$, $h_{y'} = 2\mu a'/3 = a'/3$. For these judicious mount locations, as before, the (3,1),(1,3),(3,3),(5,3),..., modes of the quadrant plates ($\mu = 1/2$) are not excited.

For the undivided plate, the fundamental resonance that occurs at the frequency ω_{11} is the most pronounced and potentially the most troublesome plate resonance encountered. Here, in Fig. 8, the severe loss in isolation observed at the frequency ω_{11} has been mitigated by the introduction of the quadrant plates. Thus, the transmissibility peak at the fundamental resonance of the quadrants ($\Omega \approx 20$) lies some 13.5 dB beneath the peak at the fundamental resonance of the undivided plate ($\Omega \approx 6$), even though it remains essentially as "abrupt" as before.

Peak values of transmissibility can also be reduced effectively by attaching dynamic vibration absorbers to the undivided plate, for example, at all four mount locations. One such dynamic absorber is shown in the broken area of Fig. 9(a). The four dynamic absorbers have identical design, and each comprises a lumped mass M_a that is connected by a spring of stiffness K_a and a dashpot having a coefficient of viscosity η_a to the plate, the motion of which is excessive at some resonant frequency that, in this instance, is taken to be ω_{11}. The absorbers are tuned to resonate at a frequency neighboring ω_{11} at which their motion becomes relatively large, whereas the motion of the plate and the force transmitted to its boundaries are minimized. The absorbers have natural frequencies $\omega_a = (K_a/M_a)^{1/2}$ and damping ratios $\delta_R = (\eta_a/\eta_{ac}) = (\omega_a\eta_a/2K_a)$, where η_{ac} is the value of the coefficient of viscosity required to damp the absorbers critically.[2]

The force transmissibility across the mounting system of Fig. 9(a) (Introduction) can be expressed as follows:

$$T = \left| \frac{T^*}{\{[1 - (\Omega^*)^2](1 - \gamma_a \xi^* \theta^*) - \gamma \xi^*\}} \right| \quad , \tag{40}$$

where Ω^*, γ, T^*, and ξ^* are given by Eqs. 6, 14, 23, and 24, and

$$\theta^* = \frac{(1 + j\Delta_a)}{[1 - \Omega_m^2(\omega_{11}/\omega_a)^2 + j\Delta_a]} \quad . \tag{41}$$

In these equations

$$\gamma_a = 4M_a/M_p \quad , \tag{42}$$

$$\Delta_a = 2(\omega_{11}/\omega_a)\Omega_m\delta_R \quad , \tag{43}$$

and

$$\Omega_m = \frac{\omega}{\omega_{11}} = \frac{(\omega/\omega_o)}{(\omega_{11}/\omega_o)} = \frac{\Omega}{\Xi} \quad , \tag{44}$$

where Ω and Ξ are again related by Eq. 19. The so-called tuning ratio ω_a/ω_{11} and the damping ratio δ_R are design parameters of the dynamic absorbers, and the choice of suitable values for them is important if the full effectiveness of the absorbers is to be realized. The values chosen in this situation are those determined previously for a single absorber[7] attached to the midpoint of a rectangular plate that is driven centrally by a vibratory point force. Although four dynamic absorbers are now attached to a plate that is driven simultaneously by four noncentral point forces, the absorber tuning and damping ratios established previously[7] have been found to yield very satisfactory results in the present situation. (Note that the tuning and damping ratios should relate to an absorber of mass M_a, not $4M_a$. For example, if $\gamma_a = 4M_a/M_p = 0.2$, the appropriate values of $\omega_a/\omega_{11} = 0.869$ and $\delta_R = 0.268$ are those tabulated in Ref. 7 for an absorber of mass $M_a = 0.05\ M_p$ that is attached to a rectangular plate of aspect ratio $\mu = 1/2$. Equally massive absorbers attached to square plates, and to rectangular plates of other aspect ratios, would employ similar values of ω_a/ω_{11} and δ_R.)

The effectiveness of the dynamic absorbers is illustrated in Fig. 10, where the dashed curve relates to the transmissibility across the mounting system of Fig. 1(b) supported by a rectangular plate for which $\gamma = 6$, $\Xi = 5$, and $\mu = 1/2$. The four antivibration mounts are again located judiciously where $h_x/a = h_y/\mu a = 1/3$. The solid curve predicts the transmissibility across a duplicate mounting system to which four dynamic absorbers have been attached in the manner of Fig. 9(a). The absorbers have the mass ratio $\gamma_a = 0.2$, so that the appropriate values of ω_a/ω_{11} and δ_R are those specified in the foregoing. Although each absorber has only five percent of the plate mass, the absorbers are highly effective in suppressing the fundamental plate resonance to which they are tuned. In fact, the transmissibility peak where $\Omega \approx 6$ has essentially been suppressed by a factor of ten in magnitude. Moreover, as observed previously for foundation beams with clamped terminations,[6] the relatively large damping ratio of the absorbers is also markedly effective in suppressing the plate resonances at higher frequencies, particularly those adjoining ω_{11}. It is encouraging that the practical design of absorbers to suppress resonant floor motion has been discussed in Refs. 8 and 9.

Finally, it is instructive to consider plates that are mass loaded at each mount location, as in Fig. 9(b). The transmissibility in this case follows readily from Eq. 40 when it is recognized that the dynamic absorbers of Fig. 9(a) will degenerate into lumped masses M_a if the absorber springs or dampers are made infinitely stiff or viscous. In either case, the parameter $\theta^* = 1.0$ in Eq. 41. No other modification is required. Representative calculations of transmissibility appear in the final Fig. 11, where the dashed curve shows the transmissibility across the basic mounting system of Fig. 1(b) for which $\mu = 1/2$. Once again, $\gamma = \Xi = 4$, and the antivibration mounts are judiciously located where $h_x/a = h_y/\mu a = 1/3$. The transmissibility across an identical mounting system to which lumped masses have been added at each mount location, as in Fig. 9(b) is shown by the solid curve. The total added mass is equal to that of the mounted item of machinery; namely, $\gamma_a = 4M_a/M_p = 4$. Use of such heavy mass loading is necessary if the overall level of the transmissibility curve is to be reduced significantly. For a value of $\gamma_a = 1.0$, the resultant transmissibility curve would lie approximately halfway between the solid and dashed curves at frequencies above the fundamental plate resonance ($\Omega \approx 3$). Adoption of a mass ratio as small as 0.2 -- that of the dynamic absorbers utilized previously -- would be ineffectual in reducing transmissibility much below the level of the dashed curve, except at very high frequencies where the impedance of the loading masses M_a would eventually predominate the plate impedance.

The masses M_a shift the plate resonances and the accompanying transmissibility peaks to lower frequencies, as the solid curve ($\gamma_a = 4$) of Fig. 11 indicates. Such a frequency shift, which is always apparent when a structure is mass loaded,[2,6,7] has the detrimental effect here of increasing the level of the transmissibility peak at the frequency ω_{11}

of the fundamental plate resonance. However, at higher frequencies, adoption of the substantial mass ratio has provided very large reductions in transmissibility. In fact, no transmissibility peaks are evident (within the dB range considered) once the frequency ratio $\Omega > 88$. Although the use of quadrant plates would yield considerably fewer transmissibility peaks than presently appear in the dashed curve of Fig. 11, it should be recognized that, for the quadrant plates, the transmissibility would follow the level of the dashed curve rather than the greatly reduced level of the solid curve for the mass-loaded plate of Fig. 9(b).

ACKNOWLEDGMENTS

The assistance of Adah A. Wolfe in obtaining the results presented graphically in this paper is acknowledged with gratitude. The investigation was sponsored jointly by the U. S. Naval Sea Systems Command and the U. S. Office of Naval Research.

REFERENCES

1. Symbols with a star superscript denote complex quantities; symbols with a superior tilde denote sinusoidally varying quantities.

2. J. C. Snowdon, Vibration and Shock in Damped Mechanical Systems (John Wiley and Sons, Inc., New York, 1968).

3. R. L. Kerlin and J. C. Snowdon, "Driving-Point Impedances of Cantilever Beams -- Comparison of Measurement and Theory," J. Acoust. Soc. Am. 47, 220-228 (1970).

4. J. B. Ochs and J. C. Snowdon, "Transmissibility Across Simply Supported Thin Plates: I, Rectangular and Square Plates with and without Damping Layers," J. Acoust. Soc. Am. 58, 832-840 (1975).

5. J. C. Snowdon, "Forced Vibration of Internally Damped Rectangular and Square Plates with Simply Supported Boundaries," J. Acoust. Soc. Am. 56, 1177-1184 (1974).

6. J. C. Snowdon, "Isolation of Machinery Vibration from Nonrigid Substructures Using Multiple Antivibration Mountings," contribution to Isolation of Mechanical Vibration, Impact, and Noise, edited by J. C. Snowdon and E. E. Ungar (American Society of Mechanical Engineers, New York, September, 1973) Chap. 5, pp. 102-127.

7. J. C. Snowdon, "Vibration of Simply Supported Rectangular and Square Plates to which Lumped Masses and Dynamic Vibration Absorbers are Attached," J. Acoust. Soc. Am. 57, 646-654 (1975).

8. K. H. Lenzen, "Vibration of Steel Joist-Concrete Slab Floors," AISC Eng. J., 3, 133-136 (1966).

9. D. L. Allen and J. C. Swallow, "Annoying Floor Vibrations -- Diagnosis and Therapy," Sound and Vib. Mag. 9, No. 3, 12-17 (1975).

FIGURE LEGENDS

Fig. 1 Rectangular plates with simply supported boundaries, mass M_p, and sides of lengths a and μa. A vibrating item of machinery of mass M is supported (a) by eight, and (b) by four, symmetrically located antivibration mounts, each of complex stiffness K^*.

Fig. 2 Force transmissibility across the mounting system of Fig. 1(a) supported by a square plate ($\mu = 1.0$). Antivibration mounts are uniformly spaced such that $h_{1x} = 0.2a$, $h_{1y} = \mu a/3 = a/3$, and $h_{2x} = 0.4a$, $h_{2y} = a/3$. Mass ratio $\gamma = M/M_p = 4$; frequency ratio $\Xi = \omega_{11}/\omega_o = 4$; mount and plate damping factors $\delta_K = 0.05$ and $\delta_E = \delta_G = 0.01$.

Fig. 3 Force transmissibility across the mounting system of Fig. 1(b) supported by a square plate. Antivibration mounts are located such that $h_x = h_y = 0.25a$. The parameters $\gamma = \Xi = 4$, $\delta_K = 0.05$, and $\delta_E = \delta_G = 0.01$.

Fig. 4 Force transmissibility across the mounting system of Fig. 1(b) supported by a square plate. Antivibration mounts are judiciously located such that $h_x = h_y = a/3$. The parameters $\gamma = \Xi = 4$, $\delta_K = 0.05$, and $\delta_E = \delta_G = 0.01$.

Fig. 5 (a) A circular plate, and (b) a rectangular plate divided into quadrants. The plates have simply supported boundaries and mass M_p. The circular plate of radius a' is excited by forces from four antivibration mounts symmetrically located at a distance $\lambda a'$ from the plate center. The identical quadrant plates, which have sides of lengths a' and $\mu a'$, are likewise excited by forces from four symmetrically located antivibration mounts.

FIGURE LEGENDS -- CONTINUED

Fig. 6 Force transmissibility across a mounting system supported by four antivibration mounts on the circular plate of Fig. 5(a). For the solid curve ($\mu = 0.7071$), the mount locations coincide with those utilized in the calculations of Fig. 3. For the dashed curve ($\mu = 0.4414$), the mounts lie on the nodal circle of the second symmetrical plate mode, which is consequently not excited. The parameters $\gamma = \Xi = 4$, $\delta_K = 0.05$, $\nu = 1/3$, and $\delta_E = \delta_G = 0.01$.

Fig. 7 Force transmissibility across a mounting system supported by four antivibration mounts on the quadrant plates of Fig. 5(b) when $\mu = 1.0$ (square quadrants). For the solid and dashed curves ($h_{x'} = h_{y'} = a'/2$ and $2a'/3$, respectively), the mount locations coincide with those utilized in the calculations of Fig. 3 and 4. The parameters $\gamma = \Xi = 4$, $\delta_K = 0.05$, and $\delta_E = \delta_G = 0.01$.

Fig. 8 Force transmissibility across the mounting system of Fig. 1(a) supported by a rectangular plate for which $\mu = 1/2$ (solid curve). Eight antivibration mounts are uniformly spaced such that $h_{1x} = 0.2a$, $h_{1y} = \mu a/3 = a/6$, and $h_{2x} = 0.4a$, $h_{2y} = a/6$. The dashed curve shows the force transmissibility across a mounting system supported by four antivibration mounts on the quadrant plates of Fig. 5(b) when $\mu = 1/2$. The mounts are located such that $h_{x'} = 2a'/3$, $h_{y'} = 2\mu a'/3 = a'/3$. For both curves, the parameters $\gamma = 6$, $\Xi = 5$, $\delta_K = 0.05$, and $\delta_E = \delta_G = 0.01$.

Fig. 9 Vibrating item of machinery of mass M supported by four symmetrically located antivibration mounts, each of complex stiffness K^*, on rectangular plates with simply supported boundaries, mass M_p, and sides of lengths a and μa. (a) Dynamic vibration absorbers of

FIGURE LEGENDS -- CONTINUED

mass M_a, and (b) lumped loading masses M_a, are attached to the plates at each mount location.

Fig. 10 Force transmissibility across the mounting system of Fig. 9(a) supported by a rectangular plate for which $\mu = 1/2$ (solid curve). Mounts and dynamic absorbers are located such that $h_x = a/3$, $h_y = \mu a/3 = a/6$. For the dynamic absorbers, $\gamma_a = 4M_a/M_P = 0.2$, $\omega_a/\omega_{11} = 0.869$, and $\delta_R = 0.268$. The parameters $\gamma = 6$, $\Xi = 5$, $\delta_K = 0.05$, and $\delta_E = \delta_G = 0.01$. The dashed curve shows the transmissibility across the same mounting system when the absorbers are absent ($\gamma_a = 0$).

Fig. 11 Force transmissibility across the mounting system of Fig. 9(b) supported by a rectangular plate for which $\mu = 1/2$ (solid curve). Mounts and lumped masses are located such that $h_x = a/3$, $h_y = \mu a/3 = a/6$. The parameters $\gamma_a = 4M_a/M_P = 4$, $\gamma = \Xi = 4$, $\delta_K = 0.05$, and $\delta_E = \delta_G = 0.01$. The dashed curve shows the transmissibility across the same mounting system when the loading masses are absent ($\gamma_a = 0$).

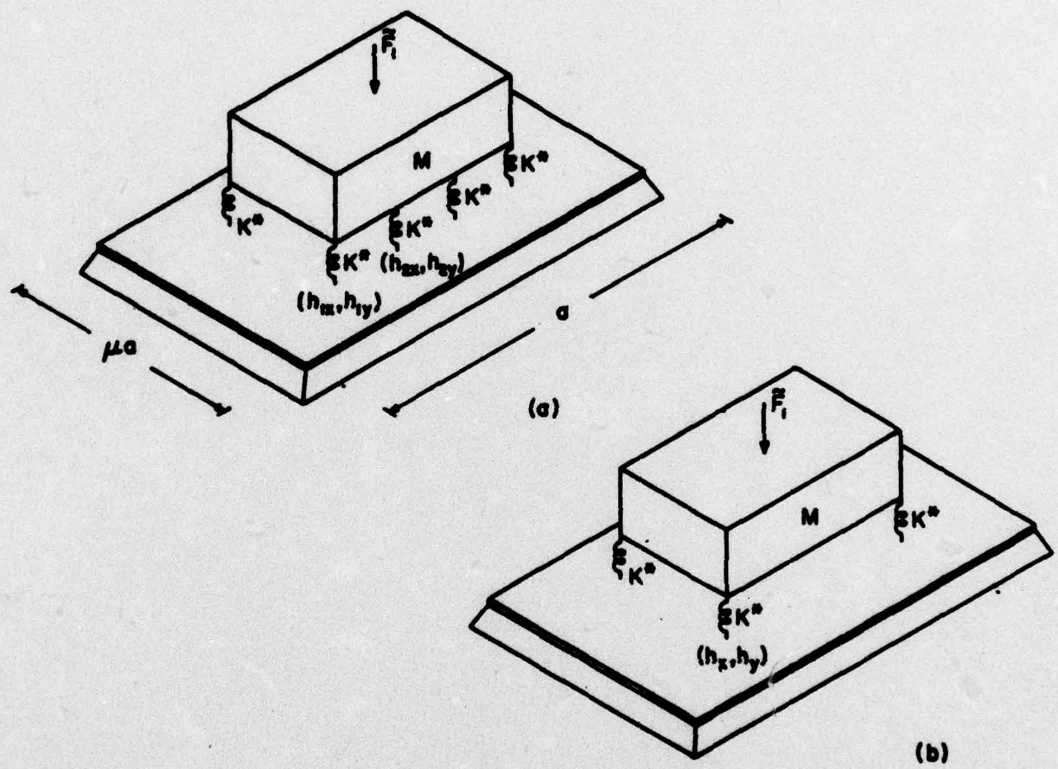

FIG. 1

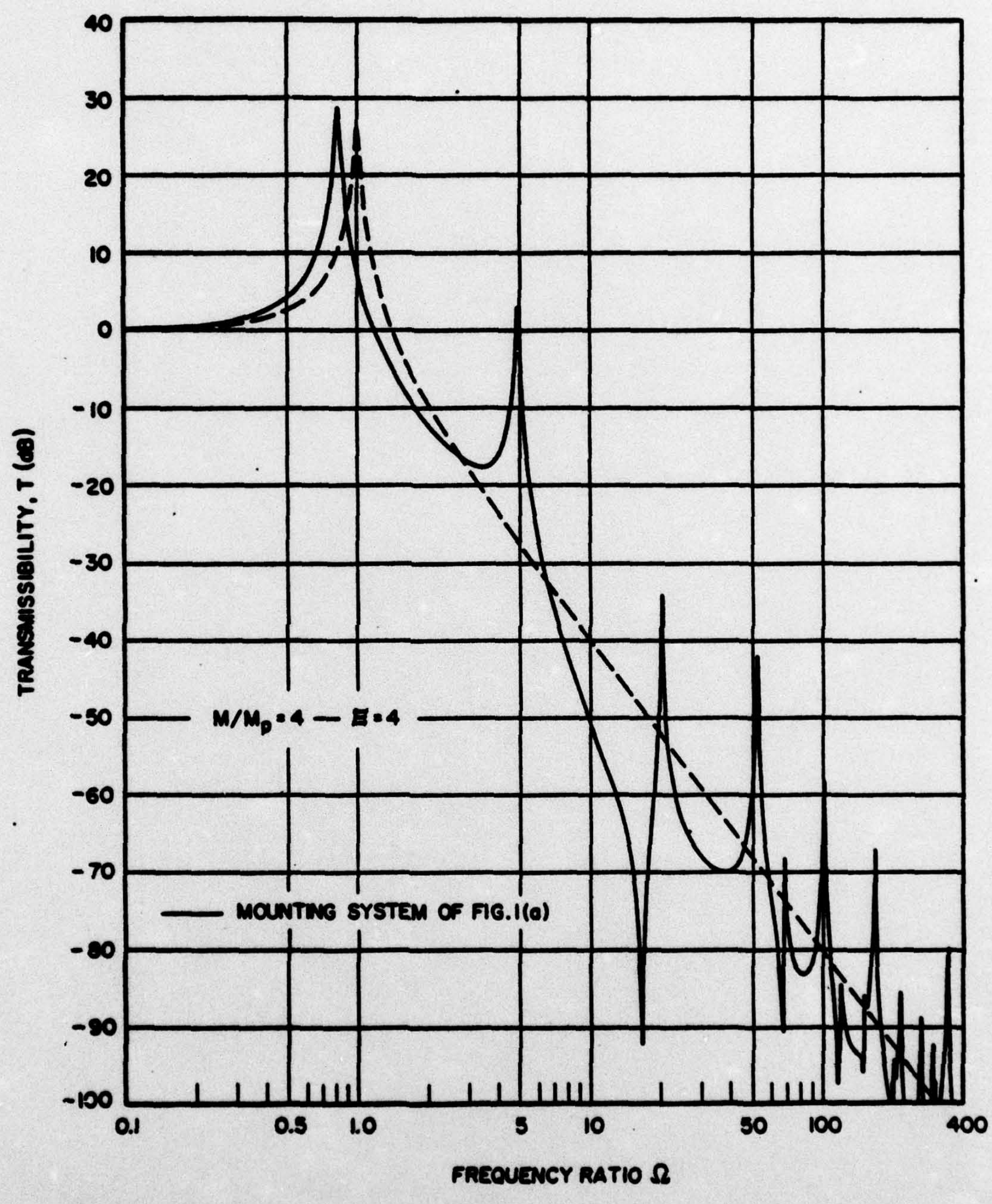
40
30
20
10
0
-10
-20
-30
-40
-50
-60
-70
-80
-90
-100
TRANSMISSIBILITY, T (dB)
M/Mp = 4 — Ξ = 4
MOUNTING SYSTEM OF FIG.1(a)
0.1
0.5
1.0
5
10
50
100
400
FREQUENCY RATIO Ω

FIG. 2

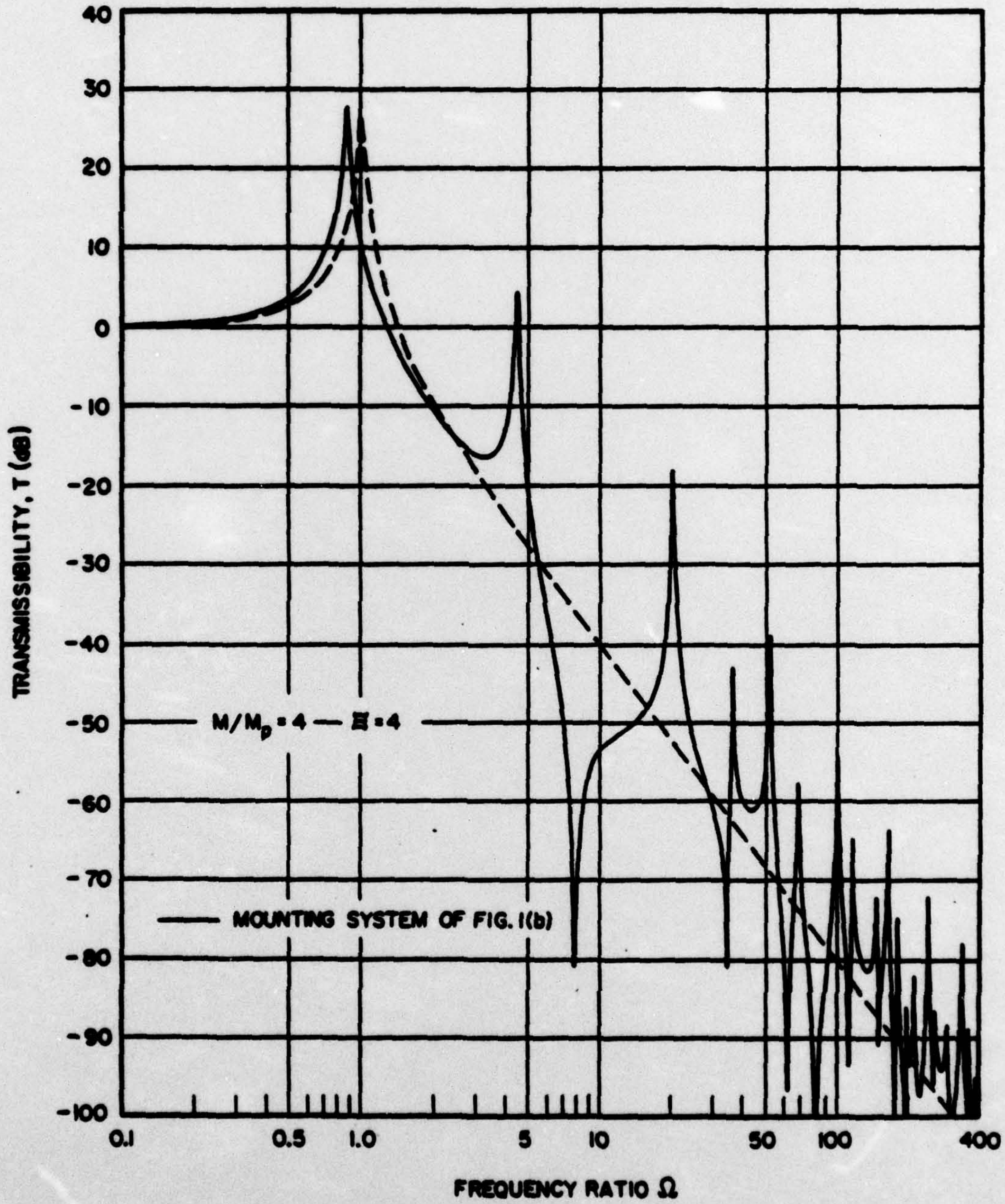
40
30
20
10
0
-10
-20
-30
-40
-50
-60
-70
-80
-90
-100
TRANSMISSIBILITY, T (dB)
M/Mp = 4 — Ξ = 4
MOUNTING SYSTEM OF FIG. 1(b)
0.1
0.5
1.0
5
10
50
100
400
FREQUENCY RATIO Ω

FIG. 3

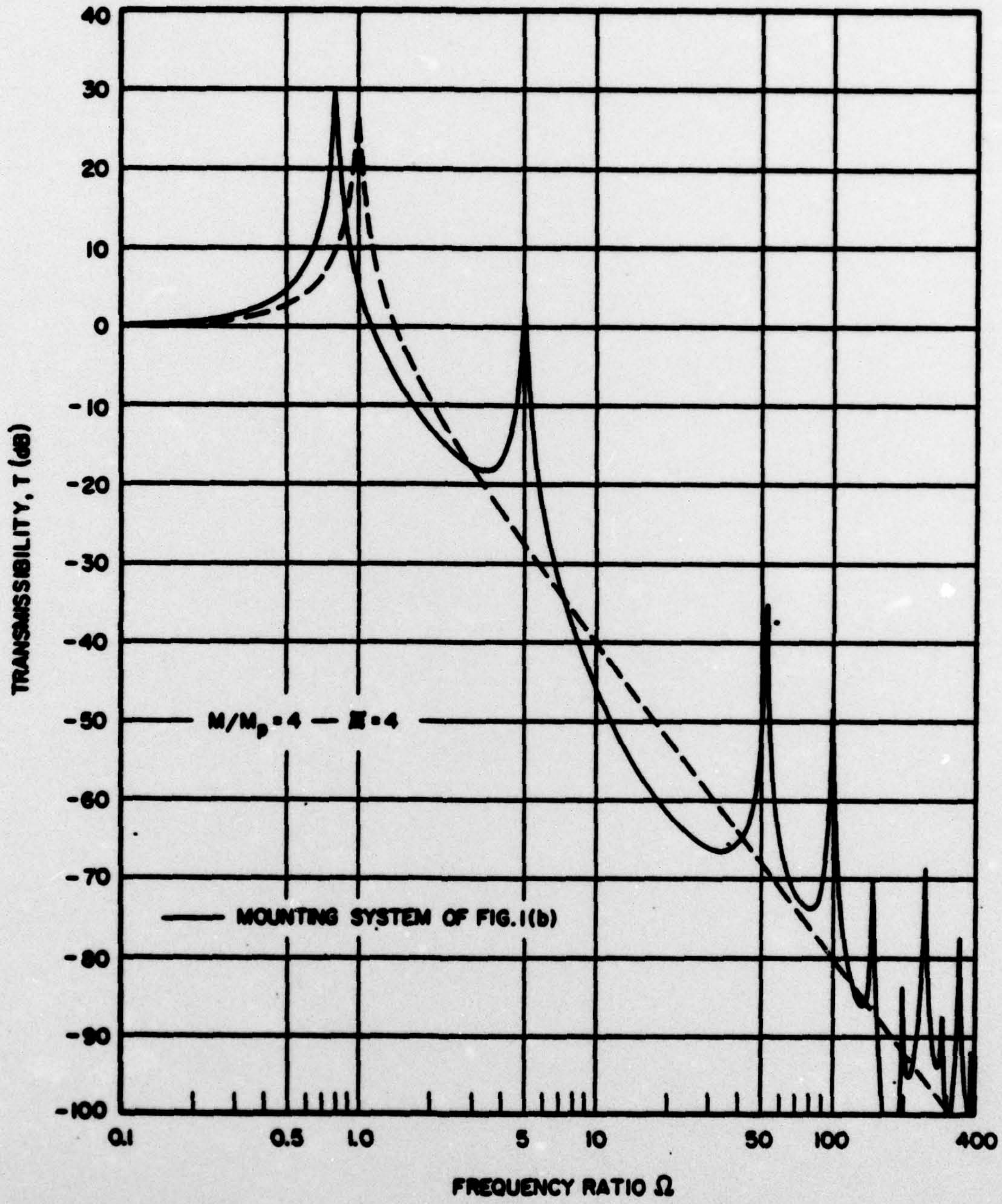

40
30
20
10
0
-10
-20
-30
-40
-50
-60
-70
-80
-90
-100
TRANSMISSIBILITY, T (dB)
$M/M_p = 4$
MOUNTING SYSTEM OF FIG. 1(b)
0.1
0.5
1.0
5
10
50
100
400
FREQUENCY RATIO Ω

FIG. 4

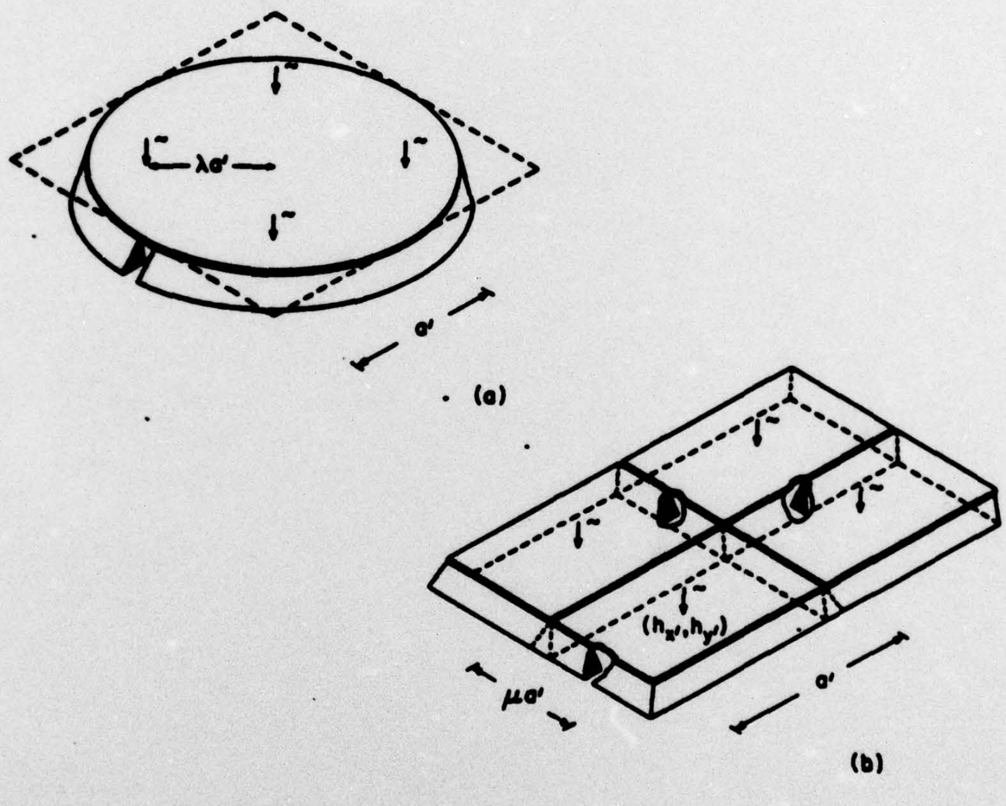

FIG. 5

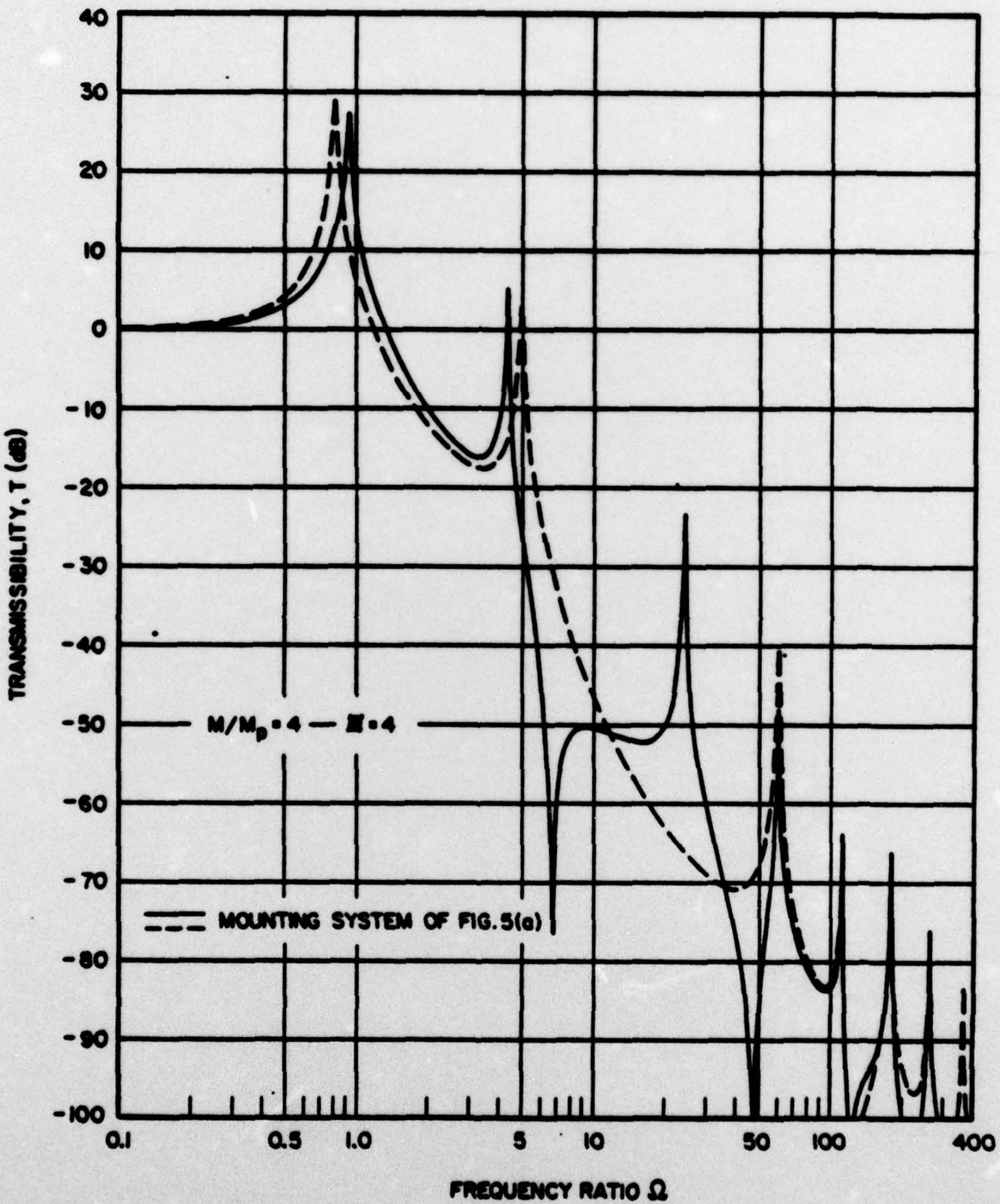

40
30
20
10
0
-10
-20
-30
-40
-50
-60
-70
-80
-90
-100
TRANSMISSIBILITY, T (dB)
M/Mp = 4 — Ⅲ = 4
MOUNTING SYSTEM OF FIG. 5(a)
0.1
0.5
1.0
5
10
50
100
400
FREQUENCY RATIO Ω

FIG. 6

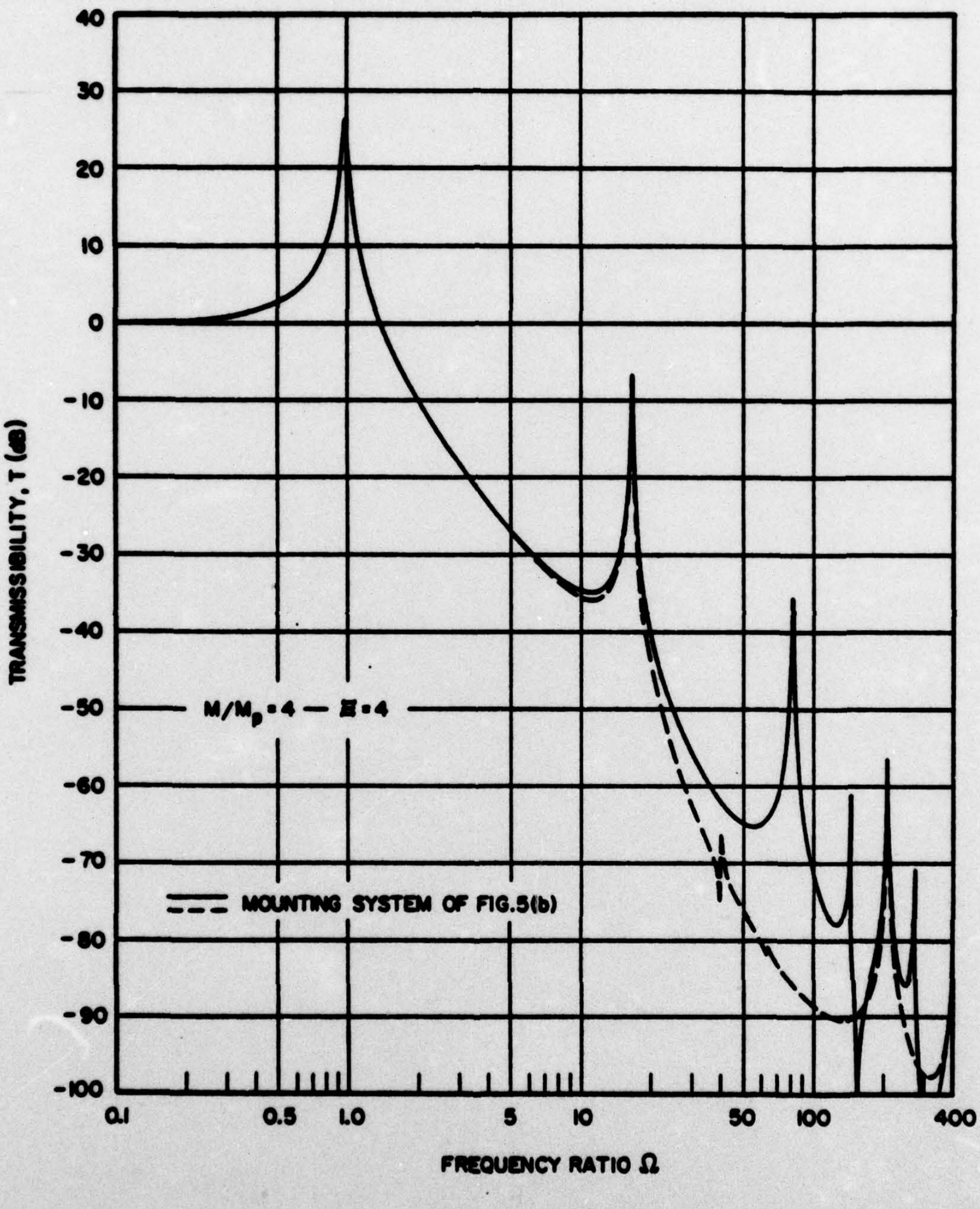

40
30
20
10
0
-10
-20
-30
-40
-50
-60
-70
-80
-90
-100
TRANSMISSIBILITY, T (dB)
M/Mp = 4 — Ξ = 4
MOUNTING SYSTEM OF FIG.5(b)
0.1
0.5
1.0
5
10
50
100
400
FREQUENCY RATIO Ω

FIG.7

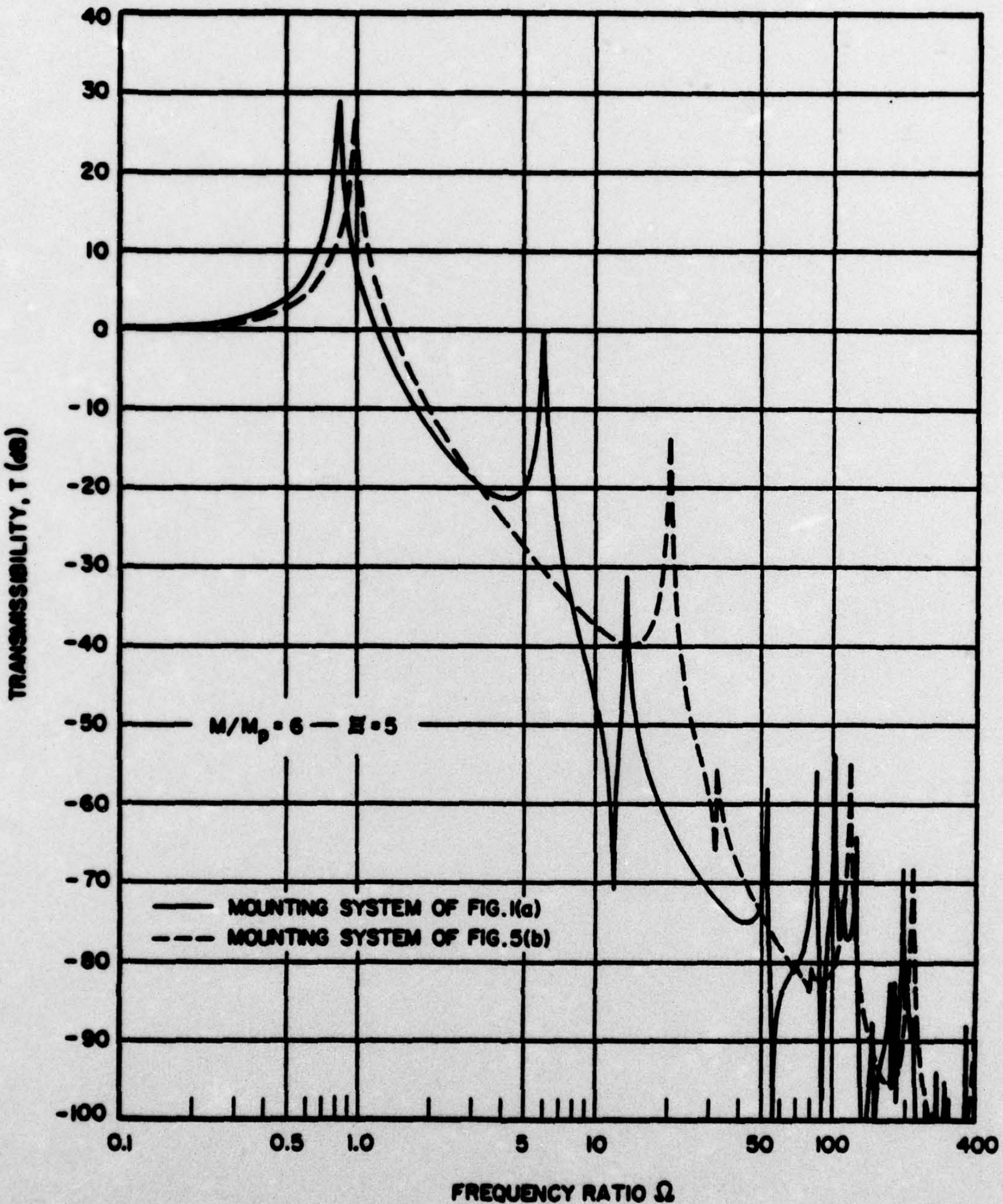
40
30
20
10
0
-10
-20
-30
-40
-50
-60
-70
-80
-90
-100
TRANSMISSIBILITY, T (dB)
M/Mp = 6 — Ξ = 5
MOUNTING SYSTEM OF FIG.1(a)
MOUNTING SYSTEM OF FIG.5(b)
0.1
0.5
1.0
5
10
50
100
400
FREQUENCY RATIO Ω

FIG.8

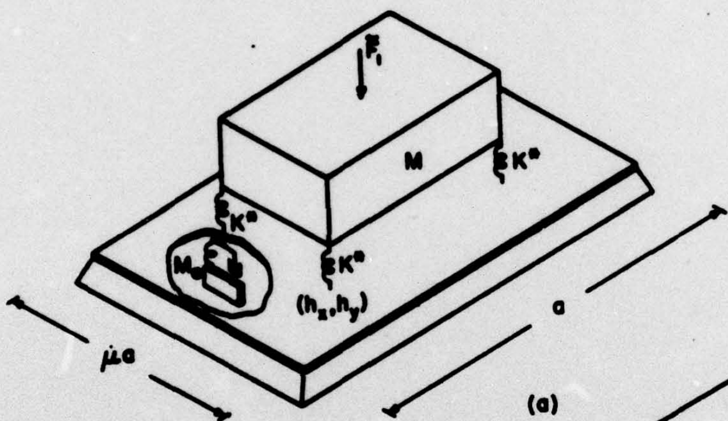

(a)

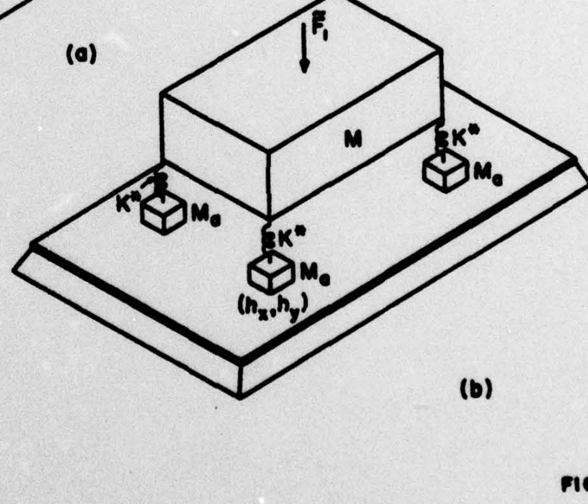

(b)

FIG. 9

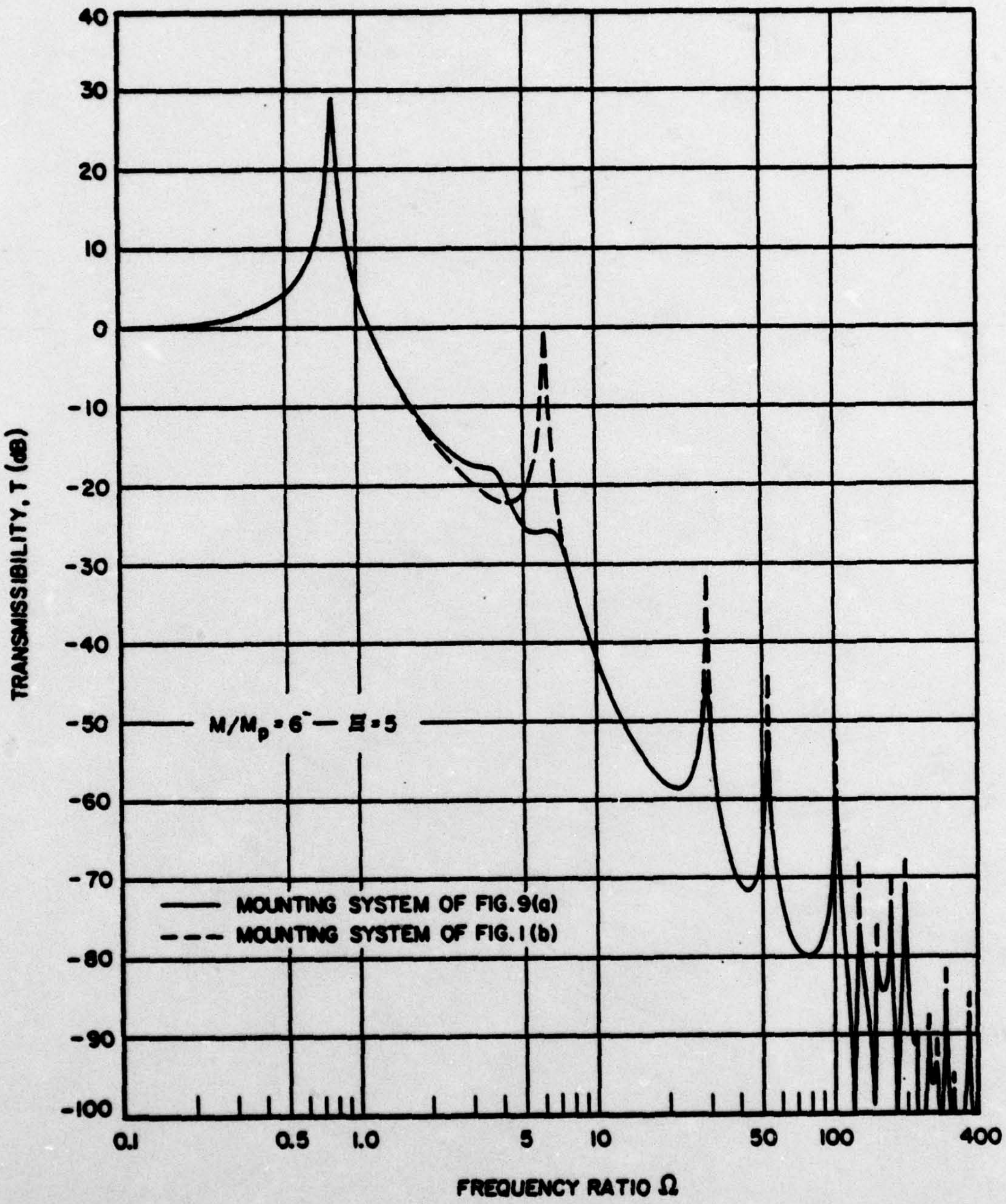

40
30
20
10
0
-10
-20
-30
-40
-50
-60
-70
-80
-90
-100
TRANSMISSIBILITY, T (dB)
M/Mp = 6 — Ξ = 5
MOUNTING SYSTEM OF FIG. 9(a)
MOUNTING SYSTEM OF FIG. 1(b)
0.1
0.5
1.0
5
10
50
100
400
FREQUENCY RATIO Ω

FIG. 10

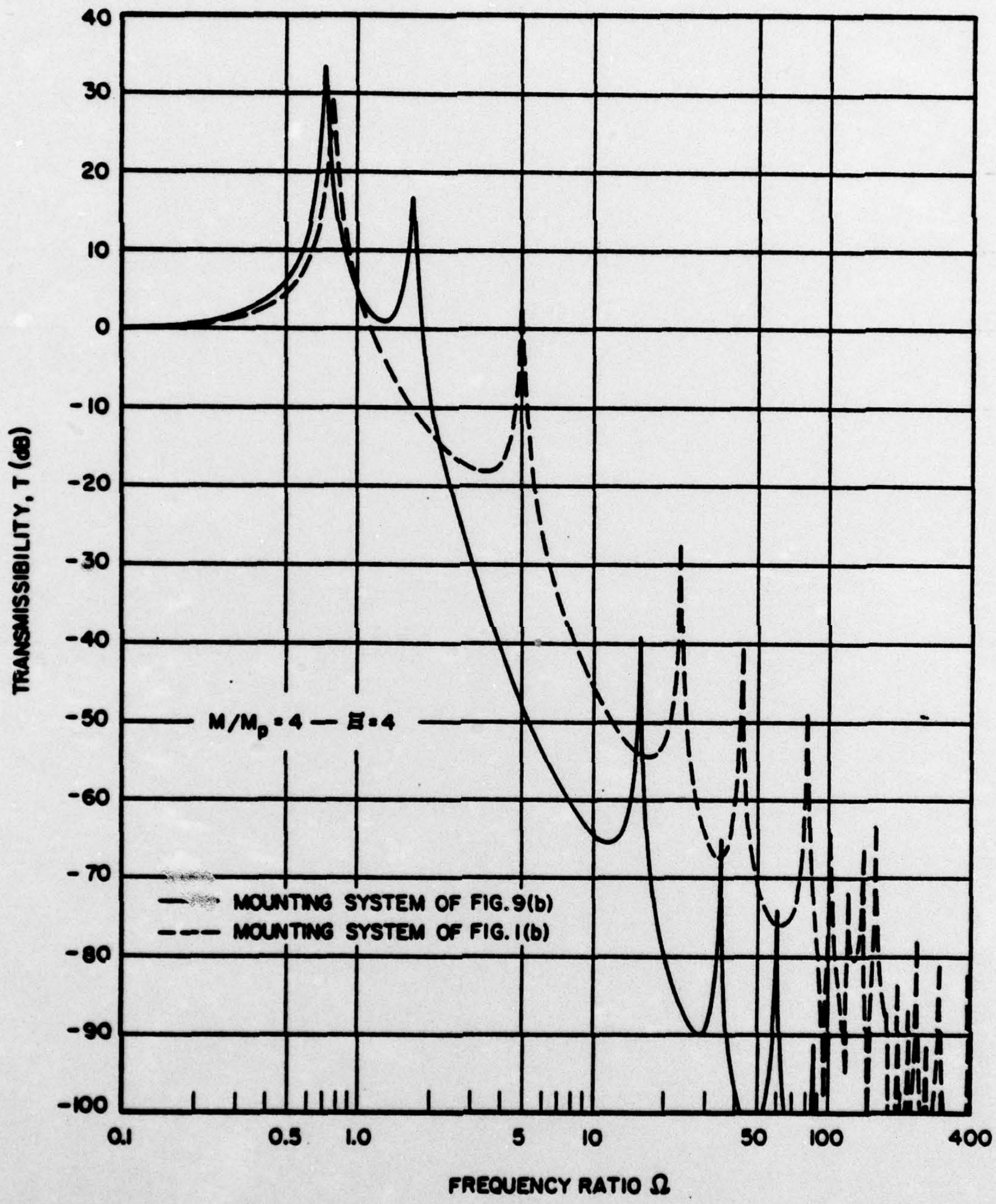
40
30
20
10
0
-10
-20
-30
-40
-50
-60
-70
-80
-90
-100
TRANSMISSIBILITY, T (dB)
M/M$_p$ = 4 — Ξ = 4
MOUNTING SYSTEM OF FIG. 9(b)
MOUNTING SYSTEM OF FIG. 1(b)
0.1
0.5
1.0
5
10
50
100
400
FREQUENCY RATIO Ω

FIG. 11

DISTRIBUTION LIST FOR UNCLASSIFIED TM 76-278

Commander
Naval Sea Systems Command
Department of the Navy
Washington, DC 20362
Attn: SEA 924N
(Copy No. 1)

Commander
Naval Sea Systems Command
Department of the Navy
Washington, DC 20362
Attn: PMS-393
(Copy No. 2)

Commander
Naval Sea Systems Command
Department of the Navy
Washington, DC 20362
Attn: PMS-395
(Copy No. 3)

Commander
Naval Sea Systems Command
Department of the Navy
Washington, DC 20362
Attn: PMS-396
(Copy No. 4)

Commander
Naval Sea Systems Command
Department of the Navy
Washington, DC 20362
Attn: Mr. Stephen M. Blazek
SEA 0371
(Copy Nos. 5, 6, 7, 8)

Commander
Naval Sea Systems Command
Department of the Navy
Washington, DC 20362
Attn: Mr. Stephen G. Wieczorek
SEA 037T
(Copy Nos. 9 and 10)

Commander
Naval Sea Systems Command
Department of the Navy
Washington, DC 20362
Attn: Mr. C. C. Taylor
SEA 0372
(Copy Nos. 11 and 12)

Commander
Naval Ship Engineering Center
Center Building
Prince George's Center
Hyattsville, MD 20782
Attn: NAVSEC 6103E
(Copy Nos. 13 and 14)

Commander
Naval Ship Engineering Center
Center Building
Prince George's Center
Hyattsville, MD 20782
Attn: NAVSEC 6105C
(Copy Nos. 15 and 16)

Commander
Naval Ship Engineering Center
Center Building
Prince George's Center
Hyattsville, MD 20782
Attn: Mr. Kenneth G. Hartman
NAVSEC 6105N
(Copy Nos. 17, 18, 19, 20, 21, 22)

Commander
Naval Ship Engineering Center
Center Building
Prince George's Center
Hyattsville, MD 20782
Attn: NAVSEC 6111B
(Copy Nos. 23 and 24)

Commander
Naval Ship Engineering Center
Center Building
Prince George's Center
Hyattsville, MD 20782
Attn: NAVSEC 6111D
(Copy Nos. 25 and 26)

Commander
Naval Ship Engineering Center
Center Building
Prince George's Center
Hyattsville, MD 20782
Attn: NAVSEC 6113C
(Copy Nos. 27 and 28)

Commander
Naval Ship Engineering Center
Center Building
Prince George's Center
Hyattsville, MD 20782
Attn: NAVSEC 6113D
(Copy Nos. 29 and 30)

Commander
Naval Ship Engineering Center
Center Building
Prince George's Center
Hyattsville, MD 20782
Attn: NAVSEC 6120
(Copy Nos. 31 and 32)

Commander
Naval Ship Engineering Center
Center Building
Prince George's Center
Hyattsville, MD 20782
Attn: NAVSEC 6129
(Copy Nos. 33 and 34)

Naval Ship Research and Development Center
Annapolis Division
Annapolis, MD 21402
Attn: Mr. J. Smith
(Copy No. 35)

Naval Ship Research and Development Center
Annapolis Division
Annapolis, MD 21402
Attn: Mr. L. J. Argiro
(Copy Nos. 36, 37, 38, 39, 40, 41)

Naval Ship Research and Development Center
Bethesda, MD 20084
Attn: Dr. M. Sevik
Code 19
(Copy Nos. 42 and 43)

Naval Ship Research and Development Center
Bethesda, MD 20084
Attn: Dr. W. W. Murray
Code 17
(Copy Nos. 44 and 45)

Naval Ship Research and Development Center
Bethesda, MD 20084
Attn: Dr. M. Strasberg
Code 1901
(Copy No. 46)

Naval Ship Research and Development Center
Bethesda, MD 20084
Attn: Dr. G. Maidanik
Code 1902
(Copy No. 47)

Naval Ship Research and Development Center
Bethesda, MD 20084
Attn: Dr. G. Chertock
Code 1903
(Copy No. 48)

Naval Ship Research and Development Center
Bethesda, MD 20084
Attn: Dr. D. Feit
Code 196
(Copy Nos. 49, 50, 51, 52, 53, 54)

Naval Ship Research and Development Center
Bethesda, MD 20084
Attn: Dr. J. T. Shen
Code 1942
(Copy No. 55)

Director
Defense Documentation Center
Cameron Station
Alexandria, VA 22314
(Copy Nos. 56, 57, 58, 59, 60, 61, 62. 63, 64, 65, 66, 67)

Director
Naval Research Laboratory
Washington, DC 20390
Attn: Code 8440
(Copy Nos. 68 and 69)

Ocean Structures Branch
U. S. Naval Research Laboratory
Washington, DC 20390
Attn: Dr. R. O. Belsheim
(Copy No. 70)

Office of Naval Research
Department of the Navy
Arlington, VA 22217
Attn: Dr. G. Boyer
Code 222
(Copy Nos. 71, 72, 73)

Office of Naval Research
Department of the Navy
Arlington, VA 22217
Attn: Dr. A. O. Sykes
Code 222
(Copy Nos. 74, 75, 76)

Office of Naval Research
Department of the Navy
Arlington, VA 22217
Attn: Mr. Keith M. Ellingsworth
Code 473
(Copy No. 77)

Office of Naval Research
Department of the Navy
Arlington, VA 22217
Attn: Dr. N. Perrone
Code 474
(Copy No. 78)

Commander
Mare Island Naval Shipyard
Vallejo, CA 94592
(Design Division)
(Copy No. 79)

Commander
Portsmouth Naval Shipyard
Portsmouth, NH 03801
(Copy No. 80)

Supervisor of Shipbuilding,
Conversion and Repair
General Dynamics Corporation
Electric Boat Division
Groton, CT 06340
Attn: Dr. Robert M. Gorman
Dept. 440
(Copy Nos. 81 and 82)

Supervisor of Shipbuilding,
Conversion and Repair
Ingalls Shipbuilding Corporation
Pascagoula, MS 39567
(Copy No. 83)

Supervisor of Shipbuilding,
Conversion and Repair
Newport News Shipbuilding and Drydock Company
Newport News, VA 23607
(Copy No. 84)

Naval Ship Research and
Development Center
Underwater Explosion Research
Division
Code 780
Portsmouth, VA 23709
(Copy No. 85)

Naval Underwater Systems Center
New London Laboratory
New London, CT 06320
Attn: Mr. G. F. Carey
(Copy No. 86)

Naval Underwater Systems Center
New London Laboratory
New London, CT 06320
Attn: Dr. R. S. Woollett
(Copy No. 87)

Naval Undersea Warfare Center
San Diego, CA 92152
Attn: Mr. G. Coleman
(Copy No. 88)

Dr. J. Barger
Bolt Beranek and Newman, Inc.
50 Moulton Street
Cambridge, MA 02138
(Copy No. 89)

Dr. D. I. G. Jones
Air Force Materials Laboratory
Wright-Patterson Air Force Base
Ohio 45433
(Copy No. 90)

Dr. M. C. Junger, President
Cambridge Acoustical Associates, Inc.
1033 Massachusetts Avenue
Cambridge, MA 02138
(Copy No. 91)

Acquisitions Supervisor
Technical Information Service
American Institute of Aeronautics
and Astronautics, Inc.
750 Third Avenue
New York, NY 10017
(Copy No. 92)

Dr. R. S. Ayre
Department of Civil Engineering
University of Colorado
Boulder, CO 80302
(Copy No. 93)

Dr. D. Frederick
Chairman, Engineering Science and Mechanics Department
Virginia Polytechnic Institute and State University
Blacksburg, VA 24061
(Copy No. 94)

Dr. D. E. Hudson
Department of Mechanics
California Institute of Technology
Pasadena, CA 91109
(Copy No. 95)

Dr. G. Herrmann, Chairman
Department of Applied Mechanics
Stanford University
Stanford, CA 94305
(Copy No. 96)

Dr. A. Kalnins
Department of Mechanical Engineering and Mechanics
Leheigh University
Bethlehem, PA 18015
(Copy No. 97)

Dr. D. D. Kana
Southwest Research Institute
8500 Culebra Road
San Antonio, TX 78206
(Copy No. 98)

Dr. Y. -H. Pao, Chairman
Department of Theoretical and Applied Mechanics
Cornell University
Ithaca
New York, NY 14850
(Copy No. 99)

Dr. J. R. Rice
School of Engineering
Brown University
Providence, RI 02912
(Copy No. 100)

Dr. P. S. Symonds
School of Engineering
Brown University
Providence, RI 02912
(Copy No. 101)

Dr. W. J. Worley
Department of Theoretical and Applied Mechanics
University of Illinois
Urbana, IL 61801
(Copy No. 102)

Dr. Dana Young
Southwest Research Institute
8500 Culebra Road
San Antonio, TX 78206
(Copy No. 103)

Commander
Naval Sea Systems Command
Department of the Navy
Washington, DC 20362
Attn: SEA-09G32-Library
(Copy Nos. 104 and 105)